Chemical Engineering Journal Advances 22 (2025) 100710

Contents lists available at ScienceDirect

Chemical Engineering Journal Advances

journal homepage: www.sciencedirect.com/journal/chemical-engineering-journal-advances

Mild reductive catalytic depolymerization of lignin in a continuous flow reactor using a Cu-enhanced Pd catalyst

Tibo De Saegher [a], Jonas Elmroth Nordlander [b], Filip Hallböök [b], Boyana Atanasova [a], Pieter Vermeir [c], Kevin M. Van Geem [d], Jeriffa De Clercq [a], An Verberckmoes [a], Christian Hulteberg [b], Jeroen Lauwaert [a,*]

[a] Industrial Catalysis and Adsorption Technology (INCAT), Department of Materials Textiles and Chemical Engineering (MaTCh), Ghent University, Valentin Vaerwyckweg 1, 9000 Ghent, Belgium
[b] Division of Chemical Engineering, Department of Process and Life Science Engineering, Lund University, SE-22100 Lund, Sweden
[c] Laboratory for Chemical Analysis (LCA), Department of Green Chemistry and Technology, Faculty of Bioscience Engineering, Ghent University, Valentin Vaerwyckweg 1, 9000 Ghent, Belgium
[d] Laboratory for Chemical Technology (LCT), Department of Materials Textiles and Chemical Engineering (MaTCh), Ghent University, Technologiepark 125, 9052 Ghent, Belgium

ARTICLE INFO

Keywords:
Heterogeneous catalysis
Continuous flow reactor
Bimetallic nanoparticle catalysts
Catalyst deactivation
Depolymerization
Lignin
Bio-aromatics

ABSTRACT

Mild reductive catalytic depolymerization (MRCD) of lignin offers a sustainable route to produce functionalized aromatic compounds. However, the economic viability is hindered by the need for expensive palladium (Pd) catalysts and the limited exploration of continuous flow reactors (CFRs), which are essential to achieve an adequate production scale. This study examines the impact of partial replacement of Pd with copper (Cu) on the performance, selectivity, active site characteristics, and deactivation of a γ-Al_2O_3 supported Pd catalyst in MRCD of lignin using a CFR. Despite containing 49 % less Pd, the PdCu catalyst achieves the same depolymerization degree as the Pd catalyst over 200 min of time on stream. During the reaction, metallic Pd is formed within the Pd catalyst and both a smaller (unordered) and larger (ordered FCC) metallic PdCu phase within the PdCu catalyst. The enhanced performance of the PdCu catalyst is attributed to synergistic effects between Pd and Cu and presence of differently sized metallic phases. A minimal impact of Cu on the selectivity, even in monomer yields, was observed. For both catalysts, the primary cause of deactivation is the hydration of the γ-Al_2O_3 support to boehmite, leading to loss of its acidity and morphological changes. Metal leaching and poisoning are insignificant, while nanoparticle growth likely arises from the reduction of the metallic phases during reaction. Only a very small amount of coke deposition is observed. Overall, the cost-effective partial replacement of Pd with of Cu forms metallic PdCu alloys during the reaction, enhancing activity without adversely affecting selectivity or deactivation.

1. Introduction

Since the identification of lignin as the most scalable and abundant resource for the sustainable production of functionalized aromatic chemicals, research towards its valorization has been ever increasing [1–4]. Global lignin production, estimated to be between 50 and 70 million tons annually and projected to grow to 225 million tons by 2030, mainly stems from the paper and pulp industry and second generation biorefineries [5–7]. However, less than 2 wt% of this lignin is currently used for production of value-added chemicals, with most of it being burned as low value fuel [5]. One of the main challenges impeding the valorization of lignin is the development of a robust, cost-effective, sustainable and selective depolymerization process to produce monomeric, dimeric and oligomeric functionalized aromatics at a commercially viable scale.

A wide range of depolymerization strategies exist, each with their own benefits and downsides. Among them, the mild reductive catalytic depolymerization (MRCD) stands out for its high selectivity, mild conditions and the use of sustainable solvents, such as water and ethanol. Additionally, MRCD can be integrated with an organosolv-like lignin

* Corresponding author.
E-mail address: Jeroen.Lauwaert@UGent.be (J. Lauwaert).

https://doi.org/10.1016/j.ceja.2025.100710

Available online 27 January 2025

extraction process, i.e., using raw biomass as a feedstock, in a process called reductive catalytic fractionation (RCF). However, two main hurdles still hinder the large-scale implementation of MRCD, and by extension RCF, for the production of lignin-derived functionalized aromatic products. The first one is the need for expensive noble metal-based catalysts, with palladium (Pd) being the most abundantly adopted, to achieve satisfactory yields towards the desired products, which limits the economic viability of the process. The incorporation of non-noble metals into the Pd-based catalysts to reduce the costs while maintaining the activity and selectivity is a relatively novel but promising route to tackle this. The addition of copper (Cu) to Pd based catalysts to boost their performance through synergetic interaction between the metals has proven successful for reactions such as the Suzuki cross coupling reaction [8–11]. Recent research has demonstrated that a PdCu catalyst can also achieve a higher activity than a Pd catalyst in the MRCD of lignin without steering the selectivity towards unwanted products, even though Cu itself is inactive at mild conditions [12,13]. However, the exact nature of the active phase during reaction, and the impact of Cu thereon, has not been studied in-depth for the MRCD or RCF. The second hurdle is that most studies on MRCD and RCF within the current literature are performed in batch reactors, while continuous flow reactors (CFRs) would provide substantial economic benefits at the production capacity of lignin and, hence, are expected to become the dominant reactor type for MRCD and RCF [14]. Especially the use of the aforementioned PdCu-based catalysts, proposed as a cost-effective solution to the first hurdle, has to the best of our knowledge, only been evaluated in batch reactors.

Therefore, this study evaluates the performance of a PdCu nanoparticle catalyst, supported on gamma alumina (γ-Al_2O_3), for the MRCD of soda lignin in a CFR. The performance of the PdCu catalyst is benchmarked against that of a comparable Pd catalyst from a recent study [13] to assess the effects of the partial replacement of Pd with Cu on three main aspects, i.e., the depolymerization performance (activity and selectivity), the nature of the active phase during reaction and the deactivation of the catalyst as a function of the time on stream (T.O.S.).

2. Materials and methods

2.1. Catalyst synthesis

The synthesis procedure for the Pd and PdCu catalysts follows a previously established method [12,13,15]. In brief, an aqueous precursor solution containing either only $Pd(NO_3)_2.2.2H_2O$ (Sigma-Aldrich, 98 %+) or both $Pd(NO_3)_2.2.2H_2O$ and $Cu(NO_3)_2.2.5H_2O$ (Chem-Lab, 98 %+) is added to γ-Al_2O_3 (Sasol Puralox sCCa 150/200) through incipient wetness impregnation at 0.75 mL of solution per 0.95 g of γ-Al_2O_3. The concentration of Pd^{2+} or Pd^{2+} and Cu^{2+} cations equates to a theoretical total metal loading of 5 wt% at a 1:1 molar ratio if two metals are present. The impregnated supports are dried at 60 °C for 16 h, heated to 450 °C at 20 °C/min and calcined at 450 °C for 4 h.

2.2. Catalyst characterization

The catalysts are characterized, before and after the catalytic tests in the CFR, using a plethora of characterization techniques, i.e., X-ray diffraction (XRD), X-ray photoelectron spectroscopy (XPS), scanning transmission electron microscopy with energy-dispersive spectroscopy (STEM-EDX), inductively coupled plasma optical emission spectroscopy (ICP-OES), nitrogen (N_2) physisorption, thermogravimetric analysis (TGA) and Fourier transform infrared spectroscopy (FT-IR). Detailed procedures for each of these techniques can be consulted in Section S1 (ESI).

2.3. Continuous flow reactor setup and depolymerization experiments

The CFR setup consists of a Salamander flow reactor (Cambridge Reactor Design) and Knauer P40 HPLC pump. A detailed description of the setup can be found in Section S2 (ESI). To perform a reaction, the lignin feed, the details of which are described in Section S3 (ESI), is pumped at 1 mL/min through the catalytic bed, consisting of 1 g of α-Al_2O_3 (Saint-Gobain) – 4 g of Pd(Cu) catalyst – 1 g of α-Al_2O_3, at 200 °C, residence time of 10 min and a back pressure between 95 – 110 bar. After equilibrating for 60 min, the effluent is collected every 2 min (2 mL) for 200 min T.O.S. The lignin feed and CFR effluents are analyzed with gel permeation chromatography with a refractive index detector (GPC-RID), two-dimensional GPC high performance liquid chromatography (GPC-HPLC-UV/VIS), phosphorous nuclear magnetic resonance spectroscopy (^{31}P-NMR) and two-dimensional heteronuclear single quantum coherence NMR (2D-HSQC-NMR). The procedures of each technique are provided in Section S4 (ESI).

3. Results and discussion

3.1. Characterization of the pristine catalysts

ICP-OES analysis of the pristine catalysts denotes 4.11 ± 0.57 wt% Pd within the Pd catalyst and 2.10 ± 0.29 wt% Pd and 1.48 ± 0.14 wt% Cu, corresponding to a molar Cu:Pd ratio of 1.18 ± 0.08, within the PdCu catalyst. The presence of Pd^{2+} in both catalysts before reaction is confirmed through XPS by the characteristic peaks at eV ($3d_{5/2}$) and eV ($3d_{3/2}$) within Figure S3 (ESI) and the corresponding PdO reflections within the XRD diffractogram in Fig. 4A. For the PdCu catalyst, no pure Cu based phases are observed within the diffractogram in Fig. 4A and the PdO related reflections, are shifted to the right through formation of a $Pd_xCu_yO_z$ phase, which is in agreement with literature [13,15–17] and Bragg's law as the incorporation of Cu cations into the Pd cation lattice leads to contraction of the unit cell. The XPS spectrum of the PdCu catalyst before reaction, Figure S4 (ESI), confirms the presence of Cu^{2+} (934.3 eV ($2p_{3/2}$), 954.4 eV ($2p_{1/2}$) and the characteristic satellite peaks) and Cu^{1+} (932.0 eV ($2p_{3/2}$) and 952.0 eV ($2p_{1/2}$)) based species. The latter was identified as Cu^{1+}, despite Cu^{1+} and Cu^0 being nearly impossible to distinguish in XPS alone [18–20], through the aforementioned XRD results. However, STEM-EDX measurements show a lower molar Cu:Pd ratio of 0.52 ± 0.20 within the nanoparticles than the global ratio derived through ICP-OES (1.18 ± 0.08). The absence of distinct Cu related reflections in XRD suggests that the excess of Cu is most likely very finely distributed across the γ-Al_2O_3 surface. This is in line with literature as previous studies have concluded that the threshold for Cu^{2+} loading of γ-Al_2O_3 without forming crystalline copper oxide phases after calcination is 0.8 mmol/100 m^2, i.e. 50 mg/100 m^2 [21–23]. In this study, the Cu^{2+} loading in the PdCu catalyst is at 18 mg/100 m^2, well below this threshold.

3.2. Effect of Cu on the depolymerization performance

The reduction in M_w, determined from GPC-RID, as a function of T.O.S. is shown in Fig. 1 for both the Pd and PdCu catalysts. The PdCu catalyst exhibits no significant difference in activity compared to Pd catalyst throughout the entire T.O.S. range, i.e., achieving the same reduction in M_w, despite containing 49 % less Pd. Moreover, as reported in previous work, Cu-γ-Al_2O_3 shows no activity at similar reaction conditions in a batch reactor [12]. Therefore, these results substantiate that the incorporation of Cu drastically enhances the activity of Pd through synergetic effects. Additionally, the Pd and PdCu-catalysts demonstrate similar degrees of deactivation, with a gradual decrease in M_w reduction as function of T.O.S.

2D-HSQC-NMR revealed that the average structural properties within the CFR effluents obtained with the Pd and PdCu catalyst also show nearly no significant differences, except at the shortest T.O.S. The total linkage and β-O-4 contents in Fig. 2A and B, are consistent with the results in Fig. 1. Similarly, the phenolic OH content (Fig. 2G) shows no significant differences across the T.O.S. range for the Pd and PdCu

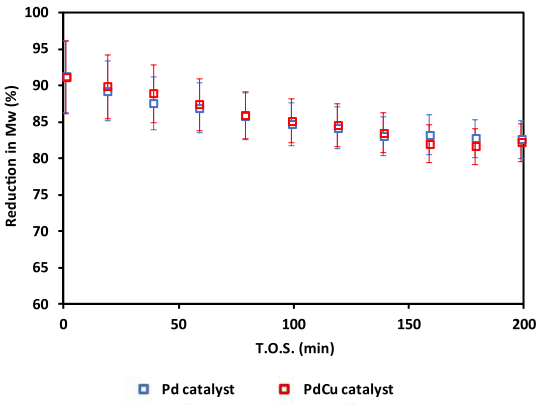

Fig. 1. Reduction in M_w as a function of T.O.S. for the Pd and PdCu catalyst experiments. Reaction conditions: 200 °C, 1 mL/min, 1 g α-Al_2O_3 – 4 g of Pd (Cu)-γ-Al_2O_3 – 1 g of α-Al_2O_3, τ = 10 min.

catalysts, further substantiating that the PdCu catalyst achieves the same degree of depolymerization as the Pd catalyst. Regarding differences in selectivity, the PdCu catalyst shows slightly higher aliphatic OH (Fig. 2H) and carboxylic acid (Fig. 2I) contents at the shortest T.O.S., indicating a very slight decrease in hydrodeoxygenation (HDO) activity compared to the Pd catalyst. However, previous research has shown that selectivity differences are mainly observable within the monomeric products [12].

The monomer yields for vanillin (V), dihydroconiferyl alcohol (DHCA), eugenol (EUG) and isoeugenol (I-EUG) in Fig. 3 reveal that while the trends for these monomers are similar, some significant differences exist between the Pd and PdCu catalysts. Noteworthy, the DHCA concentration is substantially higher at the shortest T.O.S. for the PdCu catalyst compared to the Pd catalyst (2.52 ± 0.27 wt% vs 1.50 ± 0.16 wt%), implying a lower dehydration of aliphatic hydroxyl groups. While changes in monomer yields are expected as the incorporation of Cu atoms into the Pd lattice alters adsorption [24,25], overall, the selectivity of the PdCu remains comparable to that of the Pd catalyst, despite its reduced Pd content and incorporation of Cu into the atomic lattice. This, along with the low number of significant differences in the 2D-HSQC-NMR and ^{31}P-NMR measurements, implies that the partial replacement of Pd with Cu in the PdCu catalyst did not substantially alter the reaction selectivity. However, future research into the reaction mechanisms for the Pd and PdCu catalysts could elucidate the origin of the small differences observed in Figs. 2 and 3.

3.3. Characterization of the spent catalysts

XRD (Fig. 4B) and XPS (Figure S3 (ESI)) analysis of the spent catalysts reveal that in the Pd catalyst, nearly all PdO is reduced to metallic Pd (21 nm domain size) during reaction. As no crystallite PdO is observed within the diffractogram, the remaining Pd^{2+} within the XPS spectrum (Figure S3 (ESI)) is likely due to slight oxidation of the nanoparticle surface after exposure to air. In the PdCu catalyst, the

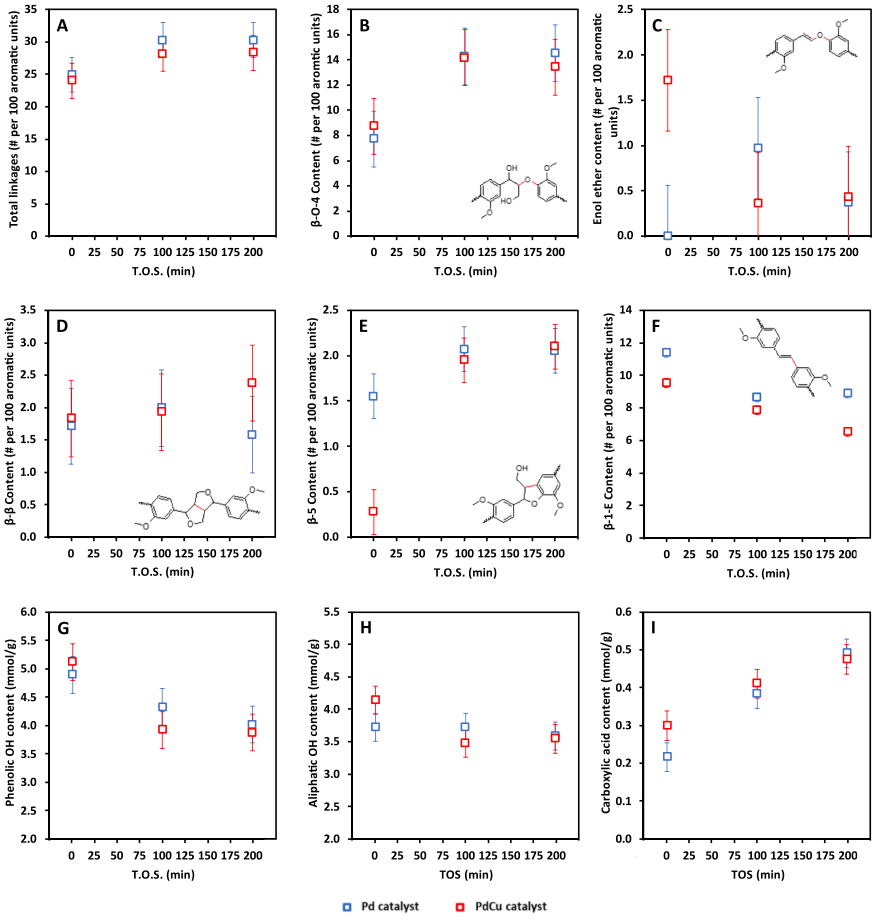

Fig. 2. 2D-HSQC-NMR derived total linkage (A), β-O-4 (B), enol ether (C), β-β (D), β-5 (E) and β-1-E (F) contents and ^{31}P-NMR derived phenolic OH (G), aliphatic OH (H) and carboxylic acid (I) contents as a function of T.O.S. for the Pd and PdCu catalyst experiments. Reaction conditions: 200 °C, 1 mL/min, 1g α-Al_2O_3 – 4 g of Pd (Cu)-γ-Al_2O_3 – 1 g of α-Al_2O_3, τ = 10 min.

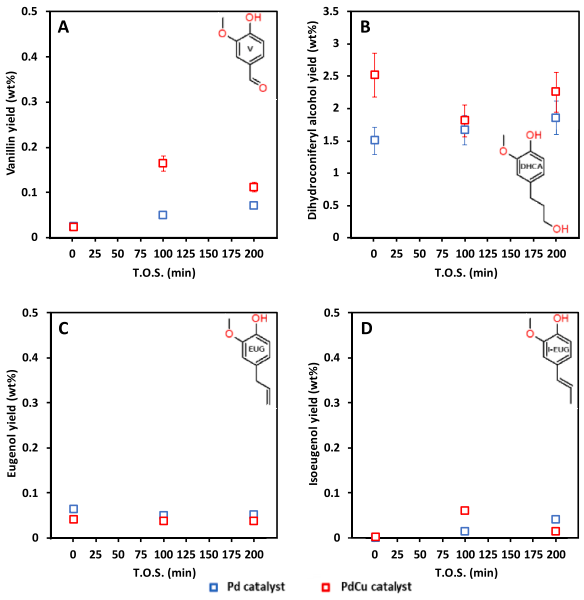

Fig. 3. GPC-HPLC-UV/VIS derived yields for vanillin (A), dihydroconiferyl alcohol (B), eugenol (C) and isoeugenol (D) as a function of T.O.S. for the Pd and PdCu catalyst experiments. Reaction conditions: 200 °C, 1 mL/min, 1g α-Al_2O_3 – 4 g of Pd(Cu)-γ-Al_2O_3 – 1 g of α-Al_2O_3, τ = 10 min.

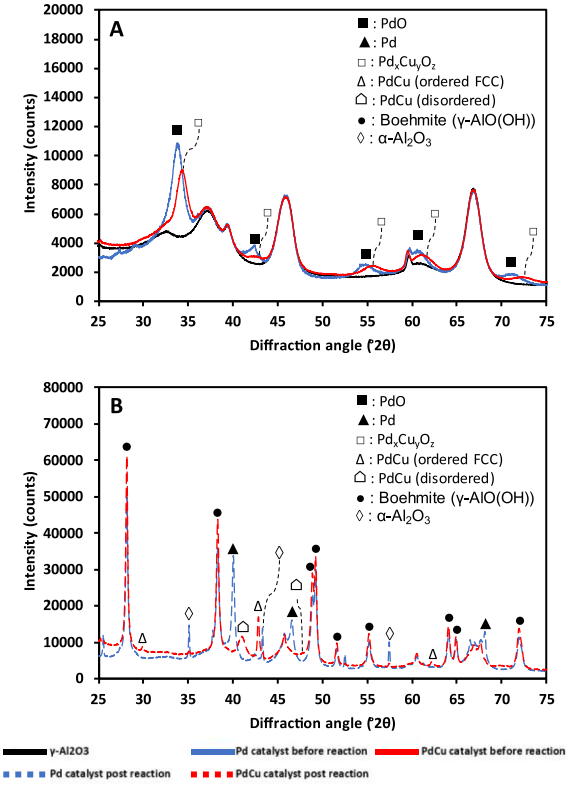

Fig. 4. XRD diffractograms for the Pd and PdCu catalysts before (A) and after (B) reaction.

aforementioned $Pd_xCu_yO_z$ phase is reduced into two distinct metallic PdCu alloys, i.e., an ordered FCC alloy phase with reflections at 30°, 43° and 57.5° (domain size of 42 nm, see Section S1.1 in ESI) and an unordered lattice with reflections at 41° and 47° (domain size of 9 nm). The XPS spectrum in Figure S4 (ESI) confirms this as the Cu^{2+} related (satellite) peaks are no longer present after reaction. As only metallic PdCu alloys are observed within the XRD data, any Cu^{1+} related species, that cannot be differentiated from metallic Cu in XPS alone, are also attributed to slight oxidation of the nanoparticle surface. While Pd oxides are known to reduce under very mild conditions [26–29], the reduction of the Cu^{2+} species in the PdCu catalyst during reaction, i.e., under an environment typically too mild for the reduction of copper oxides, is likely facilitated by Pd, as previously reported in literature [30,31].

Some studies suggest that smaller nanoparticles exhibit higher activities [32] in MRCD while others indicate that multidentate adsorption of lignin molecules on larger nanoparticles drastically boosts activity [33]. The formation of both a smaller and larger PdCu phase, compared to the metallic Pd phase in the Pd catalyst, may therefore partially explain why the PdCu catalyst achieves the same depolymerization degree as the Pd catalyst despite having a much lower Pd content. Additionally, the presence of a metallic PdCu phase suggests potential synergistic effects that might improve the performance of the PdCu catalyst. The presence of a mixed PdCu phase before and after reaction, as well as the two PdCu alloys with different sizes is visually confirmed by the STEM-EDX mappings shown in Figure S2 (ESI). The STEM-EDX derived Cu:Pd ratio within these phases after reaction, i.e., 0.91 ± 1.20 for the ordered FCC phase and 0.97 ± 0.53 for the unordered lattice, match up to the ICP-OES derived global Cu:Pd ratio of 1.02 ± 0.07. This implies that most of the Cu initially dispersed across the γ-Al_2O_3 surface in the pristine catalyst, most likely the Cu^{2+} related species noted in Section 3.1, is incorporated within the metallic PdCu alloys through migration induced by the ability of Pd to facilitate the reduction of Cu [16,34–37]. While in-situ characterization techniques such as STEM-EDX and XPS would be required to fully confirm that these metallic PdCu alloy phases are the truly active phases, as well as elucidate how they are being formed and/or change during reaction, these results are an insightful first step into identifying the reasons behind the improved performance of the PdCu catalyst over that of the Pd catalyst.

Five main modes of deactivation were assessed using various catalyst characterization techniques to investigate the effect of Cu on the deactivation behavior of Pd. Firstly, ICP-OES analysis indicated no significant leaching of either Pd (2.10 ± 0.29 wt% to 2.54 ± 0.29 wt%) or Cu (1.48 ± 0.14 wt% to 1.55 ± 0.16 wt%) for the PdCu catalyst. As no Pd leaching was observed for the Pd catalyst (4.11 ± 0.57 wt% to 4.02 ± 0.57 wt%), it can be concluded that the incorporation of Cu did not negatively affect the stability of Pd on the γ-Al_2O_3 surface.

Secondly, both in the pristine and spent PdCu catalysts, no significant amounts of sulfur (S) or sodium (Na) were detected using STEM-EDX, see Table S2 (ESI). This lack of significant poisoning in the PdCu catalyst is in line with the results obtained for the Pd catalyst [13] and implies that the addition of Cu did not influence poisoning.

Thirdly, the nanoparticle size distributions (NSDs) in Fig. 5A–D, reveal that the nanoparticle size increases significantly during the lignin depolymerization experiment for both the Pd (from 8.74 ± 1.19 nm to 16.70 ± 0.88 nm) and PdCu catalysts (from 6.24 ± 0.78 nm to 10.57 ± 0.82 nm). This nanoparticle growth can be due to reaction induced sintering and/or the phase change described in Section 3.2. Nonetheless, the PdCu catalyst shows significantly smaller nanoparticles before as well as after reaction, and also less nanoparticle growth (69.46 ± 10.22 % vs 91.19 ± 13.35 %) than the Pd catalyst, implying an increased stability.

Fourthly, phase degradation of the γ-Al_2O_3 support to boehmite during the CFR experiment has been identified as the main method of deactivation for the Pd catalyst in previous work. This degradation is also observed for the PdCu catalyst in XRD with the boehmite reflections at 28°, 38°, 49°, 49.3°, 52°, 55°, 64°, 65° and 72° in Fig. 4B. Rietveld analysis, see Figure S5 (ESI), reveals full conversion of γ-Al_2O_3 to boehmite for both the Pd and PdCu catalyst. Additionally, adsorption bands related to symmetric/asymmetric Al-O-H bending (1068 cm^{-1}/1156 cm^{-1}) and Al-OH stretching (3090 cm^{-1}/3308 cm^{-1}) in boehmite are observed in the FT-IR spectra of both the Pd and PdCu catalyst, see Fig. 5E after reaction. Furthermore, N_2 physisorption data points

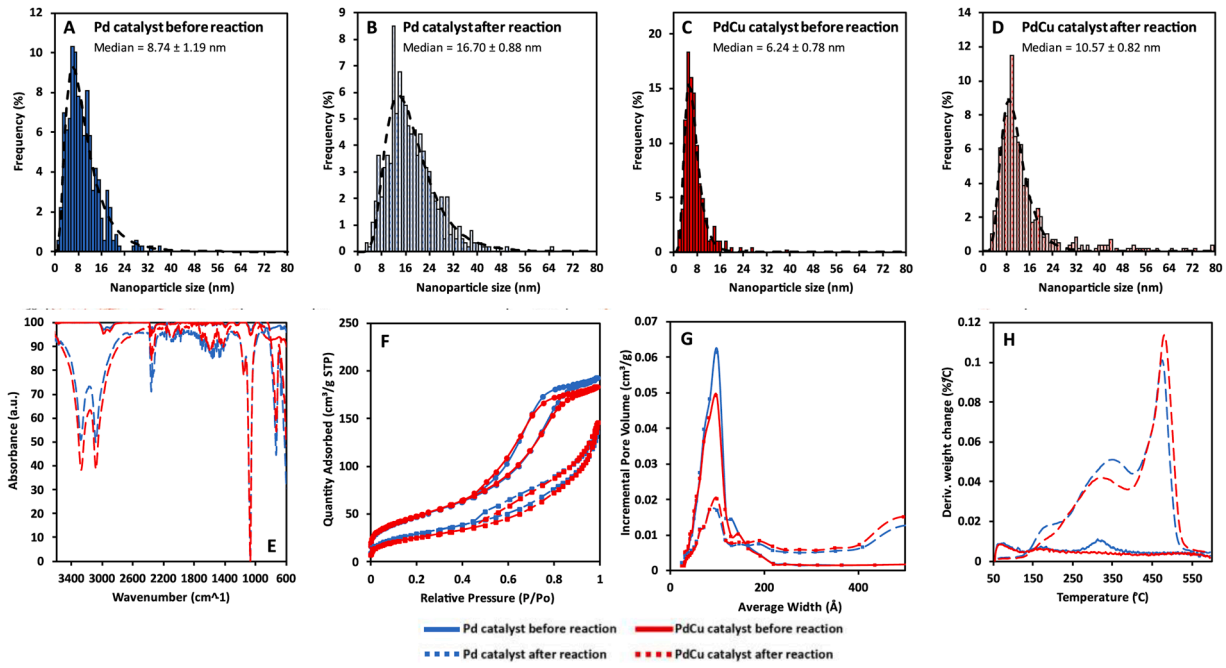

Fig. 5. Nanoparticle size distributions (A-D), FT-IR spectra (E), N_2 physisorption isotherms (F), pore size distributions (G) and TGA derivative weight change (H) for the Pd and PdCu catalysts before and after reaction.

towards a decrease of the specific surface area (172 m^2/g to 107 m^2/g for Pd and 175 m^2/g to 93 m^2/g for PdCu) and specific pore volume (0.32 mL/g to 0.22 mL/g for Pd and 0.30 mL/g to 0.24 mL/g for PdCu) due to the change from γ-Al_2O_3 to boehmite [38]. This morphological change is substantiated by the change in N_2 physisorption isotherm from H1 Type IV before reaction to H3 type [39] after reaction in Fig. 5F, change in pore size distribution in Fig. 5G and can be confirmed visually in the STEM images in Figure S2 (ESI). On the one hand, the deactivation observed in Section 3.2 can be related to the transition from γ-Al_2O_3 to boehmite itself as it results in a loss of acidic functionalities [40–43] that can serve as cocatalysts during MRCD and changes in morphology [13, 33]. However, previous research has indicated that the acidic functionalities within the γ-Al_2O_3 support do not serve as cocatalysts for the Pd and PdCu catalysts [15]. On the other hand, it has also been noted in literature that the boehmite phase formation can lead to encapsulation of metal nanoparticles, leading to a loss of active sites in contact with the reaction environment [44]. The latter is substantiated by the significant drop in signal for Pd within the XPS spectrum after reaction, i.e., Figure S3 (ESI). The inclusion of Cu has no impact on the hydration of γ-Al_2O_3 to boehmite, which explains why the PdCu catalyst shows similar deactivation to the Pd catalyst in Fig. 1.

Finally, coke formation was not significantly noted for both the Pd and PdCu catalysts. The low intensity adsorption around 1600 cm^{-1} in the FT-IR spectra in Fig. 5E could be indicative of small amounts of coking or adsorbed water in boehmite [40,45,46]. The TGA in Fig. 5H also does not unanimously indicate coke deposition as the main mass loss around 475 °C perfectly correlates with the dehydration of boehmite to γ-Al_2O_3 [38,40] and the weight loss below 400 °C can be attributed to adsorbed and/or interstitial water within the boehmite structure [38,47,48]. In conclusion, at the worst, only very small amounts of coke deposits are present on the spent Pd and PdCu catalysts.

4. Conclusions

This study examined the impact of Cu incorporation on the activity, selectivity, nature of the active sites and deactivation of a Pd based catalyst in the MRCD of lignin on a CFR. The PdCu catalyst achieves the same depolymerization degree as the Pd catalyst, during 200 min T.O.S., despite containing about half the amount of Pd. During the reaction, metallic Pd was formed in the Pd catalyst, while the PdCu catalyst developed two distinct metallic PdCu alloy phases: a smaller unordered phase and a larger ordered FCC phase. The enhanced performance of the PdCu catalyst was attributed to synergetic effects between Pd and Cu and the presence of both smaller and larger metallic phases as compared to the Pd catalyst. Future research incorporating in-situ STEM-EDX and XPS could elucidate how these metallic PdCu alloy phases are formed and/or change during reaction. As only slight differences could be noted between the Pd and PdCu catalysts regarding selectivity, especially monomer yields, the impact of Cu thereon is minimal. Additionally, the impact of the Cu to Pd ratio during catalyst synthesis on the metallic PdCu alloys formed and, in turn, the catalytic performance of the PdCu catalyst, is another interesting topic for future research.

Finally, no significant metal leaching or poisoning was noted and the growth in nanoparticles cannot be unanimously linked to deactivation for both catalysts. The main mode for deactivation for both the Pd and PdCu catalysts is the hydration of γ-Al_2O_3 to boehmite and the resulting loss in acidic functionalities and changes in morphology. Only a small amount of coke deposition could be observed. In conclusion, the cost-effective addition of Cu to the Pd based catalyst successfully creates metallic PdCu alloys during the reaction with improved reaction performance, i.e., increased activity, no drastic changes in selectivity or negative impact on deactivation.

Funding information

T.D.S. and B.A. are doctoral researchers funded by the Research Foundation Flanders (FWO, Grants 1SD8723 N and 1S15125 N). The authors also express their gratitude for additional financial support provided by the FWO through Grant V463323 N.

CRediT authorship contribution statement

Tibo De Saegher: Writing – original draft, Visualization, Validation, Software, Methodology, Investigation, Funding acquisition, Formal analysis, Data curation, Conceptualization. **Jonas Elmroth Nordlander:** Writing – review & editing, Visualization, Methodology,

Investigation, Formal analysis, Data curation. **Filip Hallböök:** Writing – review & editing, Visualization, Methodology, Investigation, Formal analysis, Data curation. **Boyana Atanasova:** Writing – review & editing, Visualization, Validation, Investigation, Formal analysis, Data curation. **Pieter Vermeir:** Writing – review & editing, Resources. **Kevin M. Van Geem:** Writing – review & editing, Supervision, Funding acquisition. **Jeriffa De Clercq:** Writing – review & editing, Supervision, Resources, Funding acquisition, Conceptualization. **An Verberckmoes:** Writing – review & editing, Supervision, Resources, Project administration, Funding acquisition, Conceptualization. **Christian Hulteberg:** Writing – review & editing, Supervision, Resources, Project administration, Funding acquisition, Conceptualization. **Jeroen Lauwaert:** Writing – review & editing, Supervision, Resources, Project administration, Methodology, Funding acquisition, Conceptualization.

Declaration of competing interest

The authors declare that they have no known competing financial interests or personal relationships that could have appeared to influence the work reported in this paper.

Acknowledgements

T.D.S. and B.A. are doctoral researchers funded by the Research Foundation Flanders (FWO, Grants 1SD8723 N and 1S15125 N). The authors also express their gratitude for additional financial support provided by the FWO through Grant V463323 N. (S)TEM-EDX and SEM-EDX analyses were carried out by Vitaliy Bliznuk at the UGent TEM Core Facility. We also extend our thanks to the INSTALAB core facility at Ghent University for their analytical services and access to equipment. Special appreciation is given to Tove Kristensen for assistance with TGA and N_2 physisorption, and to Selda Bekirovska, Lucy Ajakaiye Jensen, and Mariona Battestini Vives for their help with the reactor setup.

Supplementary materials

Supplementary material associated with this article can be found, in the online version, at doi:10.1016/j.ceja.2025.100710.

Data availability

Data will be made available on request.

References

[1] S. Kim, S.C. Chmely, M.R. Nimlos, Y.J. Bomble, T.D. Foust, R.S. Paton, G. T. Beckham, Computational study of bond dissociation enthalpies for a large range of native and modified lignins, J. Phys. Chem. Lett. 2 (2011) 2846–2852, https://doi.org/10.1021/jz201182w.

[2] M. Witzler, A. Alzagameem, M. Bergs, B. El Khaldi-Hansen, S.E. Klein, D. Hielscher, B. Kamm, J. Kreyenschmidt, E. Tobiasch, M. Schulze, Lignin-derived biomaterials for drug release and tissue engineering, Molecules. 23 (2018), https://doi.org/10.3390/molecules23081885.

[3] W. Schutyser, T. Renders, S. Van den Bosch, S.-F. Koelewijn, G. Beckham, B. Sels, Chemicals from lignin: an interplay of lignocellulose fractionation, depolymerisation, and upgrading, Chem. Soc. Rev. 47 (2018), https://doi.org/10.1039/C7CS00566K.

[4] P. Bruijnincx, B. Weckhuysen, G.-J. Gruter, E. Engelen-Smeets, Lignin_valorisation: the importance of a full value chain approach, 2016.

[5] M.Erfani Jazi, G. Narayanan, F. Aghabozorgi, B. Farajidizaji, A. Aghaei, M. A. Kamyabi, C.M. Navarathna, T.E. Mlsna, Structure, chemistry and physicochemistry of lignin for material functionalization, SN. Appl. Sci. 1 (2019) 1094, https://doi.org/10.1007/s42452-019-1126-8.

[6] EPA, Inventory of US Greenhouse Gas Emissions and Sinks, EPA Washington, DC, 2017. https://www.epa.gov/ghgemissions/inventory-us-greenhouse-gas-emissions-and-sinks-1990-2017 (accessed August 15, 2024).

[7] D.S. Bajwa, G. Pourhashem, A.H. Ullah, S.G. Bajwa, A concise review of current lignin production, applications, products and their environmental impact, Ind. Crops. Prod. 139 (2019) 111526, https://doi.org/10.1016/j.indcrop.2019.111526.

[8] X. Hu, P. Han, W. Zhang, T. Li, M. Liu, Y. Wu, Catalytic property and synergistic effect of the multi-active sites Pd/PdO/Er2O3/Cu2O/PdCu3 formed in situ on the surface of the tri-organometallic Pd(II)/Er(III)/Cu(II) film, Molec. Catal. 568 (2024) 114486, https://doi.org/10.1016/j.mcat.2024.114486.

[9] N. Li, D. Huang, T. Li, M. Liu, Y. Wu, Nano-multiactive sites Pd/PdO/CuO/PdCu3 formed In situ on the surface hetero-organometallic Pd(II)/Cu(II) nanosheet: investigation on the formation of active sites, synergistic, and catalytic activity, Appl. Organomet. Chem. (2024), https://doi.org/10.1002/aoc.7817.

[10] D. Huang, Q. An, L. Wang, T. Li, M. Liu, Y. Wu, Multi-active sites in situ formed on Schiff-base Pd(II)/Cu(II) self-assembly monolayer supported on graphene oxide: A simple protocol to enhance the catalytic activity, Molec. Catal. 535 (2023) 112846, https://doi.org/10.1016/j.mcat.2022.112846.

[11] R. Ren, T. Li, M. Liu, Y. Wu, Fabrication and catalytic properties of "cage like" aryl imine Pd(II)/Cu(II)-bimetallic catalytic monolayer supported on graphene oxide for Suzuki coupling reaction, Chem. Eng. Sci. 253 (2022) 117604, https://doi.org/10.1016/j.ces.2022.117604.

[12] T. De Saegher, B. Atanasova, P. Vermeir, K. Van Geem, J. De Clercq, A. Verberckmoes, J. Lauwaert, Enhancing the performance of heterogeneous palladium based catalysts in the mild reductive depolymerization of Soda lignin through addition of a non-noble metal and tuning of the preparation strategy, RSC Sustain. (2024), https://doi.org/10.1039/D4SU00054D.

[13] T. De Saegher, J. Elmroth Nordlander, F. Hallböök, B. Atanasova, P. Vermeir, K. M. Van Geem, J. De Clercq, A. Verberckmoes, C. Hulteberg, J. Lauwaert, Heterogeneously catalyzed lignin depolymerisation in continuous flow: assessing feedstock pretreatment and catalyst deactivation, Chem. Eng. J. 503 (2025) 158216, https://doi.org/10.1016/j.cej.2024.158216.

[14] E. Cooreman, T. Vangeel, K. Van Aelst, J. Van Aelst, J. Lauwaert, J.W. Thybaut, S. Van den Bosch, B.F. Sels, Perspective on overcoming scale-up hurdles for the reductive catalytic fractionation of lignocellulose biomass, Ind. Eng. Chem. Res. 59 (2020) 17035–17045, https://doi.org/10.1021/acs.iecr.0c02294.

[15] B. Atanasova, T. De Saegher, H. Poelman, A. de Reviere, J. Vercammen, A. Verberckmoes, J. De Clercq, J. Lauwaert, Pd catalysts in the mild reductive depolymerization of soda lignin: support and Cu addition effects, Chem. Eng. J. 498 (2024) 155866, https://doi.org/10.1016/j.cej.2024.155866.

[16] Q. Zhao, J. Wang, X. Huang, Y. Yao, W. Zhang, L. Shao, Copper-enriched palladium-copper alloy nanoparticles for effective electrochemical formic acid oxidation, Electrochem. commun. 69 (2016) 55–58, https://doi.org/10.1016/j.elecom.2016.05.021.

[17] R. Khobragade, P. Dahake, N. Labhsetwar, G. Saravanan, A PdCu nanoalloy catalyst for preferential CO oxidation in the presence of hydrogen, New J. Chem. 45 (2021) 4246–4252, https://doi.org/10.1039/D1NJ00005E.

[18] J.A. Torres-Ochoa, D. Cabrera-German, O. Cortazar-Martinez, M. Bravo-Sanchez, G. Gomez-Sosa, A. Herrera-Gomez, Peak-fitting of Cu 2p photoemission spectra in Cu0, Cu1+, and Cu2+ oxides: a method for discriminating Cu0 from Cu1+, Appl. Surf. Sci. 622 (2023) 156960 https://doi.org/10.1016/j.apsusc.2023.156960.

[19] J.F. Moulder, J. Chastain. Handbook of X-ray Photoelectron Spectroscopy: A Reference Book of Standard Spectra For Identification and Interpretation of XPS DataPhysical Electronics Division, Perkin-Elmer Corporation 275, 1992.

[20] T.M. Ivanova, K.I. Maslakov, A.A. Sidorov, M.A. Kiskin, R.V Linko, S.V Savilov, V. V Lunin, I.L. Eremenko, XPS detection of unusual Cu(II) to Cu(I) transition on the surface of complexes with redox-active ligands, J. Electron. Spectros. Relat. Phenomena 238 (2020) 146878, https://doi.org/10.1016/j.elspec.2019.06.010.

[21] Q. Yu, S. Zhang, B. Yang, Dispersion of copper oxide supported on γ-alumina and its sulfation properties, Trans. Nonferr. Metals Soc. China 21 (2011) 2644–2648, https://doi.org/10.1016/S1003-6326(11)61104-7.

[22] C.M. Wang, B.Y. Zhao, Y.C. Xie, Advances in the studies of spontaneous monolayer dispersion of oxides and salts on supports, Chin. J. Catal. 24 (2003) 475–482.

[23] Y. Hu, L. Dong, J. Wang, W. Ding, Y. Chen, Activities of supported copper oxide catalysts in the NO+CO reaction at low temperatures, J. Mol. Catal. A Chem. 162 (2000) 307–316, https://doi.org/10.1016/S1381-1169(00)00299-5.

[24] I. Kumaniaev, J.S.M. Samec, Adsorption isotherms of lignin-derived compounds on a palladium catalyst, Ind. Eng. Chem. Res. 58 (2019) 6899–6906, https://doi.org/10.1021/acs.iecr.8b06159.

[25] C.W.A. Chan, A.H. Mahadi, M.M.-J. Li, E.C. Corbos, C. Tang, G. Jones, W.C.H. Kuo, J. Cookson, C.M. Brown, P.T. Bishop, S.C.E. Tsang, Interstitial modification of palladium nanoparticles with boron atoms as a green catalyst for selective hydrogenation, Nat. Commun. 5 (2014) 5787, https://doi.org/10.1038/ncomms6787.

[26] M. Sandu, V. Sidelnikov, A. Geraskin, A. Chernyavskii, I. Kurzina, Influence of the method of preparation of the Pd-Bi/Al2O3 catalyst on catalytic properties in the reaction of liquid-phase oxidation of glucose into gluconic acid, Catalysts. 10 (2020) 271, https://doi.org/10.3390/catal10030271.

[27] B. Stasinska, W. Gac, T. Ioannides, A. Machocki, Complete oxidation of methane over palladium supported on alumina modified with calcium, lanthanum, and cerium ions, J. Nat. Gas Chem. 16 (2007) 342–348, https://doi.org/10.1016/S1003-9953(08)60002-X.

[28] V.H. Sandoval, C.E. Gigola, Characterization of Pd and Pd-Pb/α-Al2O3 catalysts. A TPR-TPD study, Appl. Catal. A Gen. 148 (1996) 81–96,, https://doi.org/10.1016/S0926-860X(96)00224-4.

[29] A. Aznárez, A. Gil, S.A. Korili, Performance of palladium and platinum supported on alumina pillared clays in the catalytic combustion of propene, RSC. Adv. 5 (2015) 82296–82309, https://doi.org/10.1039/C5RA15675K.

[30] J. Batista, A. Pintar, D. Mandrino, M. Jenko, V. Martin, XPS and TPR examinations of γ-alumina-supported Pd-Cu catalysts, Appl. Catal. A Gen. 206 (2001) 113–124, https://doi.org/10.1016/S0926-860X(00)00589-5.

[31] F. Wang, G. Lu, Hydrogen feed gas purification over bimetallic Cu–Pd catalysts – effects of copper precursors on CO oxidation, Int. J. Hydrogen. Energy 35 (2010) 7253–7260, https://doi.org/10.1016/j.ijhydene.2009.12.186.

[32] J. Park, H. Setiadi, U. Mushtaq, D. Verma, D. Han, K.-W. Nam, S.K. Kwak, J. Kim, Highly efficient reductive catalytic fractionation of lignocellulosic biomass over extremely low-loaded Pd catalysts, ACS. Catal. 10 (2020) 12487–12506, https://doi.org/10.1021/acscatal.0c03393.
[33] A. Karnitski, J.-W. Choi, D.J. Suh, C.-J. Yoo, H. Lee, K.H. Kim, C.S. Kim, K. Kim, J.-M. Ha, Roles of metal and acid sites in the reductive depolymerization of concentrated lignin over supported Pd catalysts, Catal. Today 411–412 (2023) 113844, https://doi.org/10.1016/j.cattod.2022.07.012.
[34] B. Hu, Y. Yin, G. Liu, S. Chen, X. Hong, S.C.E. Tsang, Hydrogen spillover enabled active Cu sites for methanol synthesis from CO2 hydrogenation over Pd doped CuZn catalysts, J. Catal. 359 (2018) 17–26, https://doi.org/10.1016/j.jcat.2017.12.029.
[35] H. Shen, H. Li, Z. Yang, C. Li, Magic of hydrogen spillover: understanding and application, Green Energy Environ. 7 (2022) 1161–1198, https://doi.org/10.1016/j.gee.2022.01.013.
[36] S. Liu, Y. Li, N. Ta, Y. Zhou, Y. Wu, M. Li, S. Miao, W. Shen, Fabrication of palladium-copper nanoparticles with controllable size and chemical composition, J. Colloid. Interface Sci. 526 (2018) 201–206, https://doi.org/10.1016/j.jcis.2018.04.109.
[37] X. Yang, X. Zhu, R. Hou, L. Zhou, Y. Su, The promotion effects of Pd on Fe–Cu–Co based catalyst for higher alcohols synthesis, Fuel Process. Technol. 92 (2011) 1876–1880, https://doi.org/10.1016/j.fuproc.2011.05.003.
[38] S. Zanganeh, A. Kajbafvala, N. Zanganeh, M.S. Mohajerani, A. Lak, R. Bayati, H. Zargar, S.K. Sadrnezhaad, Self-assembly of boehmite nanopetals to form 3D high surface area nanoarchitectures, Appl. Physics A 99 (2010) 317–321, https://doi.org/10.1007/s00339-009-5534-2.
[39] Z. Alothman, A review: fundamental aspects of silicate mesoporous materials, Materials 5 (2012) 2874–2902, https://doi.org/10.3390/ma5122874.
[40] P. Lv, Y. Dong, Z. Wang, M. Zhang, A highly efficient Pd/boehmite catalyst for aqueous phase hydrogenation of phenol to cyclohexanone, Catal. Letters. 153 (2022) 1–8, https://doi.org/10.1007/s10562-022-04176-z.
[41] R.M. Ravenelle, J.R. Copeland, W.-G. Kim, J.C. Crittenden, C. Sievers, Structural changes of γ-Al2O3-supported catalysts in hot liquid water, ACS. Catal. 1 (2011) 552–561, https://doi.org/10.1021/cs1001515.
[42] W. Lueangchaichaweng, B. Singh, D. Mandelli, W.A. Carvalho, S. Fiorilli, P. P. Pescarmona, High surface area, nanostructured boehmite and alumina catalysts: synthesis and application in the sustainable epoxidation of alkenes, Appl. Catal. A Gen. 571 (2019) 180–187, https://doi.org/10.1016/j.apcata.2018.12.017.
[43] A. Takagaki, J.C. Jung, S. Hayashi, Solid lewis acidity of boehmite γ-AlO(OH) and its catalytic activity for transformation of sugars in water, RSC. Adv. 4 (2014) 43785–43791, https://doi.org/10.1039/C4RA08061K.
[44] T. Saelee, P. Apichoksiri, M. Rittiruam, C. Wangphon, P. Khajondetchairit, S. Praserthdam, P. Praserthdam, A density functional theory study on how γ-Al2O3 – Boehmite transformation affects carbon evolution during aqueous-phase reaction, Chemosphere 340 (2023) 139842, https://doi.org/10.1016/j.chemosphere.2023.139842.
[45] A. Paut, A. Prkić, I. Mitar, L. Guć, M. Marciuš, M. Vrankić, S. Krehula, L. Tomaško, The new ion-selective electrodes developed for ferric cations determination, modified with synthesized Al and Fe−based nanoparticles, Sensors 22 (2021) 297, https://doi.org/10.3390/s22010297.
[46] C. Morterra, C. Emanuel, G. Cerrato, G. Magnacca, Infrared study of some surface properties of boehmite (γ-AlO2H), J. Chem. Soc. Faraday Trans. 88 (1992) 339–348, https://doi.org/10.1039/FT9928800339.
[47] Y. Zhao, J. Yang, R.L. Frost, J. Kristóf, E. Horváth, Synthesis, characterization and thermal analysis of Fe-doped boehmite nanofibres and nanosheets, J. Mater. Sci. 44 (2009) 3662–3673, https://doi.org/10.1007/s10853-009-3489-5.
[48] J. Yang, R.L. Frost, Y. Yuan, Synthesis and characterization of chromium doped boehmite nanofibres, Thermochim. Acta 483 (2009) 29–35, https://doi.org/10.1016/j.tca.2008.10.024.